

Normalized Flat Minima: Exploring Scale Invariant Definition of Flat Minima for Neural Networks using PAC-Bayesian Analysis

Yusuke Tsuzuku
The University of Tokyo
RIKEN

tsuzuku@ms.k.u-tokyo.ac.jp

Issei Sato
The University of Tokyo
RIKEN

sato@k.u-tokyo.ac.jp

Masashi Sugiyama
RIKEN
The University of Tokyo
sugi@k.u-tokyo.ac.jp

Abstract

The notion of flat minima has played a key role in the generalization properties of deep learning models. However, existing definitions of the flatness are known to be sensitive to the rescaling of parameters. The issue suggests that the previous definitions of the flatness do not necessarily capture generalization, because generalization is invariant to such rescalings. In this paper, from the PAC-Bayesian perspective, we scrutinize the discussion concerning the flat minima and introduce the notion of normalized flat minima, which is free from the known scale dependence issues. Additionally, we highlight the insufficiency of existing matrix-norm based generalization error bounds. Our modified notion of the flatness does not suffer from the insufficiency, either, suggesting it better captures generalization.

1 Introduction

Theoretical understanding of the high generalization ability of deep learning models is a crucial research objective for principled improvement of the performance. Insights and formulations are also useful to compare between models and interpret them. Some prior work has explained the generalization by the fact that trained networks can be compressed well (Arora et al., 2018; Blier & Ollivier, 2018), while others have tried to explain it by the scale of the network and prediction margins (Bartlett et al., 2017; Neyshabur et al., 2018). From the minimum

description length principle (Rissanen, 1986), models representable with a smaller number of bits are expected to generalize better. Bits-back arguments (Hinton & van Camp, 1993; Honkela & Valpola, 2004) have shown that when models are stable against noise on parameters, we can describe models with fewer bits. These arguments have motivated the research on “flat minima.” Empirical work has supported the usefulness to measure the flatness on local minima (Keskar et al., 2017; Yao et al., 2018). Other work has proposed training methods to search for flatter minima (Hochreiter & Schmidhuber, 1997; Chaudhari et al., 2017; Hoffer et al., 2017). As measures of the flatness, prior work proposed the volume of the region in which a network keeps roughly the same loss (Hochreiter & Schmidhuber, 1997), the maximum loss around the minima (Keskar et al., 2017), and the spectral norm of the Hessian (Yao et al., 2018).

Despite the empirical connections of “flatness” to generalization, existing definitions of it suffer from a scale dependence issue. Dinh et al. (2017) showed that we can arbitrarily change the flatness of the loss landscape for some networks without changing the functions represented by the networks. Such scale dependence appears in networks with ReLU activation functions or normalization layers such as batch-normalization (Ioffe & Szegedy, 2015) and weight-normalization Salimans & Kingma (2016). Since generalization does not depend on rescalings of parameters, the scale dependence issue suggests that the prior definitions of “flatness” do not necessarily capture the generalization of neural networks.

What causes the problems in the previous definitions of “flatness?” In prior definitions, they implicitly used Gaussian priors with the same variance for all parameters (Sec. 3). However, as Dinh et al. (2017) pointed out, an assumption that all parameters have the same scale is not good prior knowledge for neural networks. In this paper, using a PAC-Bayesian framework (McAllester, 1999, 2003), we explicitly take scale properties of neural networks into consideration. We first incorporate the knowledge that each weight matrix can have different scales (Sec. 4). Next, we extend the analysis to row and column wise scaling of parameters (Sec. 5). To the best of our knowledge, our analysis provides the first rescaling invariant definition of the flatness of local minima. Figure 1 shows that our definition of flat minima can distinguish models trained on random labels even when a previous definition fails.

2 Related work

Neyshabur et al. (2018) analyzed the generalization of deep learning models using the PAC-Bayesian framework. They focused on bounding the worst-case propagation of perturbations. Given the existence of adversarial examples (Szegedy et al., 2014), this approach inevitably provides a loose bound. Alternatively, we rely on flat-minima arguments, which better capture the effect of parameter perturbations. We point out an additional insufficiency of their bound in Sec. 5.1. Our redefined notion of flat minima is free from this issue, suggesting it better captures generalization.

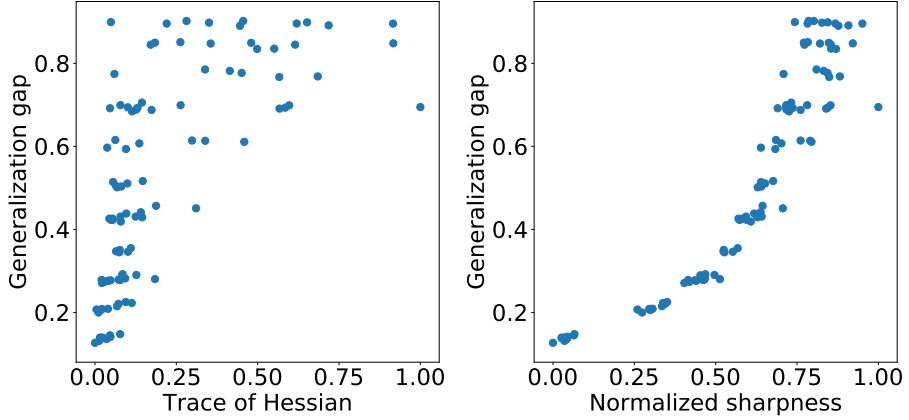


Figure 1: Scatter plot between sharpness measures and generalization gap for Wide ResNets trained on CIFAR10 with different ratio of random labels (Sec. 6). The left figure uses the trace norm of the Hessian of parameters (5) as the existing sharpness metric. The right figure uses our proposed sharpness metric: normalized sharpness (17). Both sharpness measures were rescaled to $[0, 1]$ by their maximum and minimum among the trained networks. Our modification of the notion of flat minima provides stronger correlation between the sharpness on local minima and the generalization gap. The correlation coefficient of the sharpness metrics were 70.8 and 91.1 for the trace of the Hessian and the normalized sharpness, respectively.

Wang et al. (2018) examined a better choice of the posterior variance and showed that Hessian-based analysis relates to the scale of parameters. However, their argument could not overcome the scale dependence issue. Moreover, their analysis is based on a parameter-wise argument, which involves a factor that scales with the number of parameters, making their overall bound essentially equivalent to naive parameter counting. In contrast, our analysis completely removes the scale dependence. Additionally, our analysis does not have a constant that scales with the number of parameters.

Li et al. (2018) demonstrated that normalizing the loss landscape by the scale of filters in convolutional neural networks provides better visualization of the loss landscape. While their work empirically showed the effectiveness to normalize the flatness by the scale of parameters, they did not provide theoretical justification why the normalization is essential. We provide some theoretical justifications to focus on the normalized loss landscape through the lens of the PAC-Bayesian framework.

Table 1: Notation table.

\mathbb{P} :	prior distribution of hypothesis (parameters)
\mathbb{Q} :	posterior distribution of hypothesis (parameters)
\mathcal{D} :	underlying (true) data distribution
\mathcal{S} :	training set, <i>i.i.d.</i> sample from \mathcal{D}
z_i :	i -th sample in \mathcal{S} , $z_i \in \mathcal{S}$
m :	number of data points in a training set
K :	number of class
d :	number of layers (depth) in NN
h :	number of hidden units (width) in NN
$W^{(i)}$:	i -th weight matrix
θ :	parameter of network
f :	hypothesis, typically depends on θ (f_θ)
$\mathcal{L}_\mathcal{D}(f)$:	expected (0-1) loss concerning distribution \mathcal{D}
$\mathcal{L}_z(f)$:	loss on a data point z of a hypothesis f
$\mathcal{L}_\mathcal{D}(\mathbb{Q})$:	$\mathbb{E}_{f \sim \mathbb{Q}} [\mathcal{L}_\mathcal{D}(f)]$
$\text{KL}[\mathbb{Q} \parallel \mathbb{P}]$:	KL divergence
∇_θ :	derivative concerning parameter θ
∇_θ^2 :	Hessian concerning parameter θ
$\ W\ _F$:	Frobenius norm of a matrix W
$f(z)$:	output of a hypothesis f at a data point z
$\mathbf{x}[i]$:	the i -th element of a vector \mathbf{x}
$A[i, j]$:	the (i, j) -th element of a matrix A
y_z :	label of data point z
I :	identity matrix

3 Flat minima from PAC-Bayesian perspective

In this section, we introduce a fundamental PAC-Bayesian generalization error bound and its connection to flat minima provided by prior work. Table 1 summarizes notations used in this paper.

3.1 PAC-Bayesian generalization error bound

One of the most basic PAC-Bayesian generalization error bounds is the following (Germain et al., 2016; Alquier et al., 2016).

For any distribution \mathcal{D} , any set \mathcal{H} of classifiers, any distribution \mathbb{P} of support \mathcal{H} , any $\delta \in (0, 1]$ and any positive real number λ , we have, with probability at least $1 - \delta$,

$$\mathcal{L}_\mathcal{D}(\mathbb{Q}) \leq \mathcal{L}_\mathcal{S}(\mathbb{Q}) + \lambda^{-1} (\text{KL}[\mathbb{Q} \parallel \mathbb{P}] - \ln \delta + \Psi(\lambda, m)), \quad (1)$$

where

$$\Psi(\lambda, m) := \ln \mathbb{E}_{f \sim \mathbb{P}, \mathcal{S}' \sim \mathcal{D}^m} [\exp(\lambda(\mathcal{L}_\mathcal{D}(f) - \mathcal{L}_{\mathcal{S}'}(f)))] . \quad (2)$$

We can provide calculable bounds on $\Psi(\lambda, m)$ depending on which types of loss functions we use (Germain et al., 2016). Especially when we use the 0-1 loss, $\Psi(\lambda, m)$ can be bounded by

$$\frac{\lambda^2}{2m}. \quad (3)$$

Note that this does not depend on the choice of priors. In this paper, we mainly treat the 0-1 loss.

We reorganize the PAC-Bayesian bound (1) for later use as follows.

$$\begin{aligned} \mathcal{L}_{\mathcal{D}}(f) &= \underbrace{\mathcal{L}_{\mathcal{D}}(f) - \mathcal{L}_{\mathcal{D}}(\mathbb{Q})}_{(A)} + \mathcal{L}_{\mathcal{D}}(\mathbb{Q}) \\ &\leq (A) + \mathcal{L}_{\mathcal{S}}(\mathbb{Q}) \\ &\quad + \underbrace{\lambda^{-1} \text{KL}[\mathbb{Q} \parallel \mathbb{P}]}_{(B)} + \lambda^{-1} \left(\ln \frac{1}{\delta} + \Psi(\lambda, m) \right) \\ &= (A) + (B) + \underbrace{\mathcal{L}_{\mathcal{S}}(\mathbb{Q}) - \mathcal{L}_{\mathcal{S}}(f)}_{(C)} + \mathcal{L}_{\mathcal{S}}(f) \\ &\quad + \lambda^{-1} \left(\ln \frac{1}{\delta} + \Psi(\lambda, m) \right). \end{aligned} \quad (4)$$

Similar decompositions can be found in prior work (Neyshabur et al., 2017, 2018). We use a different PAC-Bayes bound (1) for later analysis, but they are essentially the same. The original PAC-Bayesian bound (1) is for a stochastic classifier \mathbb{Q} , but the reorganized one (4) is a bound for a deterministic classifier f .

3.2 PAC-Bayesian view of flat minima

Flat minima, which are the noise stability of the training loss with respect to parameters, naturally correspond to (C) in Eq. (4). When (C) is sufficiently small, we can expect that (A) in (4) is also small. Similarly to existing work (Langford & Caruana, 2002; Arora et al., 2018; Hochreiter & Schmidhuber, 1997), we focus on analyzing terms (B) and (C).

3.3 Effect of noises under second-order approximation

To connect PAC-Bayes analysis with the Hessian of the loss landscape as prior work (Keskar et al., 2017; Dinh et al., 2017; Yao et al., 2018), we consider the second-order approximation of some surrogate loss functions. We use the unit-variance Gaussian as the posterior of parameters. Then term (C) in the

PAC-Bayesian bound (4) can be calculated as

$$\begin{aligned}
\mathcal{L}_{\mathcal{S}}(\mathbb{Q}) - \mathcal{L}_{\mathcal{S}}(f_{\theta}) &= \mathbb{E}_{\epsilon \sim \mathcal{N}(\theta, I)} [\mathcal{L}_{\mathcal{S}}(f_{\theta+\epsilon})] - \mathcal{L}_{\mathcal{S}}(f_{\theta}) \\
&\approx \mathbb{E}_{\epsilon \sim \mathcal{N}(0, I)} [\epsilon^\top \nabla_{\theta}^2 \mathcal{L}_{\mathcal{S}}(f_{\theta}) \epsilon] \\
&= \text{Tr}(\nabla_{\theta}^2 \mathcal{L}_{\mathcal{S}}(f_{\theta})) \\
&= \sum_i \nabla_{\theta_i}^2 \mathcal{L}_{\mathcal{S}}(f_{\theta}). \tag{5}
\end{aligned}$$

Thus, term (C) can be approximated by the trace norm of the Hessian. There are two issues in using the trace of the Hessian as a sharpness metric. First, we used unit-variance Gaussians for all parameters, which might not necessarily be the best choice. Second, we ignored the effect of the KL-divergence term (B). These two flaws are the keys of our analysis described in the next section.

4 Warm-up: Matrix-normalized flat minima

In this section, we modify flat minima to make them invariant to the transformations proposed in Dinh et al. (2017). Prior work has used some unit-variance Gaussian for the prior and the posterior as discussed in Sec. 3.3. This corresponds to an assumption that all parameters have the same scale. However, we already know that the scale can vary from weight matrix to weight matrix. In other words, existing choice of priors does not well capture our prior knowledge. To cope with this problem, we explicitly make parameters' priors have uncertainty in their scale. A short summary of implications in this section is that we need to multiply the scale of the loss landscape by the scale of parameters.

4.1 Controlling prior variance

In this subsection, we first revisit the technique to control the variance parameters of the Gaussian priors after training (Hinton & van Camp, 1993). Next, we consider its effect to the KL divergence term (B) in (4). Following a standard practice, we use a Gaussian with zero-mean and diagonal covariance matrix ($\sigma_{\mathbb{P}}^2 I$) where $\sigma_{\mathbb{P}} > 0$. We also use a Gaussian with mean θ and covariance $\sigma_{\mathbb{Q}}^2 I$, $\sigma_{\mathbb{Q}} > 0$ as the posterior. The mean θ is learned parameters of the network.

We first show how to control the variance parameters of the Gaussian priors after training. We introduce a hyperprior to the standard deviation $\sigma_{\mathbb{P}}$ of parameters per weight matrix¹ (Hinton & van Camp, 1993). To make the prior variance invariant to scalings, we need to use some special hyperpriors. As the hyperprior, we use a uniform prior over a finite set of real numbers². Especially,

¹We set other hyperpriors to bias terms similarly. Applying the discussion concerning weight matrices to bias terms is straightforward and thus omitted.

²Alternatively, we can use log-uniform prior over finite domain to make the prior variance invariant to scalings.

we use a set of positive numbers representable by a floating point number as the hyperprior.

To see how our hyperprior removes scale dependence from the PAC-Bayesian bound (1), we consider its effect to the KL term (B) in (4). The KL term can be written as follows.

$$\text{KL}[\mathbb{Q} \parallel \mathbb{P}] = \sum_i \ln \frac{\sigma_{\mathbb{P}}^{(i)}}{\sigma_{\mathbb{Q}}^{(i)}} + \frac{\|W^{(i)}\|_{\text{F}}^2 + (\sigma_{\mathbb{Q}}^{(i)})^2}{2(\sigma_{\mathbb{P}}^{(i)})^2} + \text{const.}, \quad (6)$$

where $W^{(i)}$ is a learned i -th weight matrix and $(\sigma_{\mathbb{P}}^{(i)})^2$ and $(\sigma_{\mathbb{Q}}^{(i)})^2$ are the prior variance and the posterior variance of the i -th weight matrix, respectively. When the prior variances are fixed, the KL term is proportional to the squared frobenius norm of parameters. However, since we introduced the special prior, we can arbitrarily change the prior variance after training and control the KL term. To minimize the KL divergence term, the prior variance $(\sigma_{\mathbb{P}}^{(i)})^2$ is set to the same value as the posterior variance $(\sigma_{\mathbb{Q}}^{(i)})^2$. Below, we use $(\sigma^{(i)})^2$ to denote both $(\sigma_{\mathbb{P}}^{(i)})^2$ and $(\sigma_{\mathbb{Q}}^{(i)})^2$. Now, thanks to our hyperprior, we can write the KL divergence term as

$$\sum_i \frac{\|W^{(i)}\|_{\text{F}}^2}{2(\sigma^{(i)})^2} + \text{const.}, \quad (7)$$

where $\sigma^{(i)}$ are parameters we can tune after training. The constant only depends on the number of weight matrices, which is much smaller than the total number of parameters. The KL divergence term (7) has additional flexibility to deal with the scale of weight matrices because we can scale $\sigma^{(i)}$ after training.

4.2 Defining matrix-normalized flat minima

In this subsection, we show how to tune the variances $(\sigma^{(i)})^2$ introduced in Sec. 4.1. Deciding the value of the variances induces our definition of scale invariant flat minima. To minimize the PAC-Bayesian bound (1), we choose the variance to minimize the following quantity.

$$\mathcal{L}_{\mathcal{S}}(\mathbb{Q}) - \mathcal{L}_{\mathcal{S}}(f) + \lambda^{-1} \text{KL}[\mathbb{Q} \parallel \mathbb{P}]. \quad (8)$$

First, we model the loss function $\mathcal{L}_{\mathcal{S}}$ by second order approximation.³ For the sake of notational simplicity, we introduce the following quantity for each weight matrix $W^{(i)}$.

$$H^{(i)} := \sum_{w \in W^{(i)}} \frac{\partial^2 \mathcal{L}_{\mathcal{S}}(f)}{\partial w \partial w}, \quad (9)$$

where w are parameters in the weight matrix. The quantity $H^{(i)}$ is the sum of the diagonal elements of the Hessian of the training loss function for the weight

³The choice of the surrogate loss function to calculate the Hessian is discussed in Sec. 5.4.

matrix $W^{(i)}$. Now, the quantity (8) can be approximated by

$$(8) \approx \sum_i \left(H^{(i)}(\sigma^{(i)})^2 + \frac{\|W^{(i)}\|_F^2}{2\lambda(\sigma^{(i)})^2} \right) + \text{const.}, \quad (10)$$

where $(\sigma^{(i)})^2$ is the the variance associated to the weight matrix $W^{(i)}$. With an assumption that the Hessian is positive semidefinite, the quantity (10) is minimized when we set

$$(\sigma^{(i)})^2 = \sqrt{\frac{\|W^{(i)}\|_F^2}{2\lambda H^{(i)}}}. \quad (11)$$

By inserting this to the quantity (10), we get

$$\sqrt{\frac{2}{\lambda} \sum_i \sqrt{\|W^{(i)}\|_F^2 H^{(i)}}} + \text{const.} \quad (12)$$

No matter what λ achieves the infimum in the PAC-Bayes bound (1), the smaller the quantity (12) is, the smaller the bound (1) is. Thus, we can use the following as a measure of generalization:

$$\sum_i \sqrt{\|W^{(i)}\|_F^2 H^{(i)}}. \quad (13)$$

We refer to this quantity as matrix-normalized sharpness. Intuitively, the sharpness is scaled by the scale of each weight matrix. Matrix-normalized sharpness (13) is invariant to the transform of parameters' scale proposed in Dinh et al. (2017). Thus, we can overcome one of the open problems by considering the effect of both terms (B) and (C) in PAC-Bayesian bound (4). Its connection to minimum description length arguments, which are the basis of flat minima arguments, is discussed in Sec. 7.1.

5 Normalized flat minima

We point out an insufficiency of matrix-wise capacity control. To address the issue, we extend matrix-normalized flat minima and define normalized flat minima. The new definition provides improved invariance while enjoying a reduced effective number of parameters in the constant term for a better generalization guarantee.

5.1 Insufficiency of matrix-wise capacity control

First, we propose a transformation different from Dinh et al. (2017) that changes the scale of the Hessian of networks arbitrarily. Let us consider a simple network with a single hidden layer and ReLU activation. We denote this network as

$$y = W^{(2)}(\text{ReLU}(W^{(1)}(x))). \quad (14)$$

We can scale the i -th column of $W^{(2)}$ by $\alpha > 0$ and i -th row of $W^{(1)}$ by $1/\alpha$ without modifying the function that the network represents as follows⁴.

$$W^{(1)}[i, :] \leftarrow \frac{W^{(1)}[i, :]}{\alpha}, \quad (15)$$

$$W^{(2)}[:, i] \leftarrow \alpha W^{(2)}[:, i]. \quad (16)$$

Since we are using the ReLU activation function, which has positive homogeneity, this transformation does not change the represented function. By the transformation, the scale of the diagonal elements of the Hessian corresponding to the i -th row of $W^{(1)}$ are scaled by α^2 . This can cause essentially the same effect with the transformation proposed by Dinh et al. (2017).

The transformation reveals an insufficiency of matrix-norm based generalization error bounds as follows. Assume $W^{(1)}$ has at least two non-zero rows and $W^{(2)}$ has at least two non-zero columns. Using the transformation, we can make both $W^{(1)}$ and $W^{(2)}$ have at least one arbitrarily large element. In other words, both weight matrices have arbitrarily large spectral norms and Frobenius norms. Also, the stable rank of the two matrices become arbitrarily close to one. Thus, the matrix-norm based capacity control (Bartlett et al., 2017; Neyshabur et al., 2018) suffers from the same rescaling dependence issue as the prior definitions of flatness.

5.2 Improving invariance of flatness

To address the newly revealed scale dependence issue in Sec. 5.1, we modify the choice of the hyperprior discussed in Sec. 4.2. We introduce a parameter σ_i for the i -th row and σ'_j for the j -th column and use the product of them as variance.⁵ In other words, we set the variance of $W_{i,j}$ to $\sigma_i \sigma'_j$. For the priors of σ and σ' , we use log-uniform priors on a constrained domain as Sec. 4. Setting the variances per row and column makes the constant term in the KL-term $O(hd)$. This is still much smaller than setting variance per parameter, which scales $O(h^2d)$. Applying the same discussion as Sec. 4.2, we define normalized sharpness as the sum of the solutions of the following optimization problem defined for each weight matrix.

$$\min_{\sigma, \sigma'} \sum_{i,j} \left(\frac{\partial^2 \mathcal{L}_S(f)}{\partial W[i, j] \partial W[i, j]} (\sigma_i \sigma'_j)^2 + \frac{W[i, j]^2}{2\lambda(\sigma_i \sigma'_j)^2} \right). \quad (17)$$

Below, we set $\lambda = 1/2$ for simpler calculation.

⁴ Running examples of the transformation can be found in Appendix A.1.

⁵ In some parameters such as bias terms and scaling parameters in normalization layers, setting variance parameters per row corresponds to applying naive parameter counting for these parameters. Thus, noise induced by the posterior become 0 and the KL-term become a constant that scales with the number of such parameters.

5.3 Practical calculation

We present a practical calculation technique to solve the optimization problem (17). First, we reparametrize variance parameters σ_i and σ'_j as follows.

$$e^{x_i} := \sigma_i^2, \quad (18)$$

$$e^{y_j} := \sigma'_j. \quad (19)$$

Fortunately, the optimization problem (17) is convex with respect to x_i and y_i .⁶ Thus, we can estimate the near optimal value of σ_i and σ'_j by gradient descent. Details of the gradient calculation can be found in Appendix C. Figure 2 shows the pseudo code of the normalized sharpness calculation.

When λ changes to λ' , the normalized sharpness (17) is scaled by $\sqrt{\lambda/\lambda'}$ as matrix-normalized flat minima (Sec. 4). Thus, networks with smaller normalized flatness at some choice of λ also have smaller normalized sharpness at other choices of λ .

In convolutional layers, since the same filter has the same scale, we only need to set the hyperprior on the input and output channels. It is straightforward to see that the convexity still holds with convolutional layers.

5.4 Choice of the surrogate loss function

When we measure the generalization gap using the 0-1 loss, which is not differentiable with respect to parameters, we need to use surrogate loss functions. The choice of the surrogate loss functions needs special care when we use flatness for model comparison. For the comparison to make sense, the value of the normalized sharpness should not change when the accuracy of the models does not change. Thus, the surrogate loss function should make the normalized sharpness invariant against at least the following changes.

1. Scaling the networks' outputs.
2. Shifting the networks' outputs.

For example, the cross entropy loss taken after softmax does not satisfy the first condition. Thus, using the loss function makes the model comparison meaningless. While the above conditions do not make the choices of the surrogate loss function unique, we heuristically use the following loss.

$$-\ln \left(\frac{\exp(f'(z)[y_z])}{\sum_i \exp(f'(z)[i])} \right), \quad (20)$$

⁶See Appendix B.

Algorithm 1 Normalized sharpness calculation

```

// Calculate diagonal elements of the Hessian
 $\mathbf{h} = \mathbb{E}_{\epsilon \sim \mathcal{N}(0,1)} \left[ \epsilon \odot \frac{\nabla_{\theta} \mathcal{L}_S(f_{\theta+r\epsilon}) - \nabla_{\theta} \mathcal{L}_S(f_{\theta-r\epsilon})}{2r} \right]$ 
// Positive semi-definite assumption might be false
 $\mathbf{h} \leftarrow \text{Clip}(\mathbf{h}, \mathbf{0})$ 
 $S \leftarrow 0$  // normalized sharpness
// Solve (17) for each weight matrix
for each weight matrix  $W^{(l)}$  do
    while not converged do
        // reparametrization to make the loss convex
         $\sigma \leftarrow \exp(\mathbf{x})$ 
         $\sigma' \leftarrow \exp(\mathbf{y})$ 
         $S^l \leftarrow 0$  // normalized sharpness of  $W^{(l)}$ 
        for each row  $i$  do
            for each column  $j$  do
                //  $\mathbf{h}^{(l)}[i, j]$  is an element of  $\mathbf{h}$ 
                // corresponding to  $W^{(l)}[i, j]$ 
                 $S^l \leftarrow S^l + \mathbf{h}^{(l)}[i, j] (\sigma[i] \sigma'[j])^2$ 
                 $S^l \leftarrow S^l + W^{(l)}[i, j]^2 / (\sigma[i] \sigma'[j])^2$ 
            end for
        end for
        SGDUpdate( $L, \mathbf{x}, \mathbf{y}$ )
    end while
     $S \leftarrow S + S^{(l)}$ 
end for
return  $S$ 

```

Figure 2: Calculation of the normalized sharpness (17).

where

$$\mu := \frac{1}{K} \sum_i f(z)[i], \quad (21)$$

$$f'(z) := \frac{f(z)}{\sqrt{\frac{1}{K} \sum_i (f(z)[i] - \mu)^2}}, \quad (22)$$

$$(23)$$

$f(z)$ is an output of a network, y_z is a label of z , and K is the number of classes. We refer to the loss function as the normalized-softmax-cross-entropy loss. This loss function is used in later experiments (Sec. 6).

6 Numerical evaluations

We numerically justify the insights from the previous sections. We specifically investigate the followings.

- Whether normalized sharpness (Sec. 5) distinguish models trained on random labels (Sec. 6.1).
- Whether normalized sharpness better captures generalization than existing sharpness metrics (Sec. 6.2).

Detailed experimental setups are described in Appendix E.

6.1 Normalized sharpness to distinguish models trained on random labels

We checked whether normalized sharpness can distinguish models trained on random labels. Hypothesis which fit random labels belong to hypothesis classes such that Rademacher complexity is 1. Thus, if normalized sharpness captures generalization reasonably well, it should have a larger value for networks trained on random labels.

Quantities: We investigated the correlation between normalized sharpness (17) and generalization gap defined by (train accuracy – test accuracy). Sharper minima is expected to have larger generalization gap. A loss function (20) was used as the surrogate loss function of 0-1 loss.

Set up: We trained a multilayer perceptron with three hidden layers and LeNet (Lecun et al., 1998) on MNIST (LeCun et al., 1998) and LeNet and Wide ResNet (Zagoruyko & Komodakis, 2016) with 16 layers and width factor 4 on CIFAR-10 (Krizhevsky, 2009) for 100 times for each pair. At each run, we randomly selected the ratio of random labels from 0 to 1 at 0.1 intervals. We used Adam optimizer and applied no regularization or data augmentation so that the training accuracy reached near 1 even with random labels.

Results: Figure 3 shows scatter plots of normalized sharpness v.s. accuracy gap for networks trained on MNIST and CIFAR-10. The results show that networks tended to have larger normalized sharpness to fit random labels. Thus, we can say that normalized sharpness provides reasonably good hierarchy in hypothesis class. These results support our analysis concerning normalized flat minima in Sec. 4 and Sec. 5.

6.2 Effect of normalization

We tested how our modification of flat minima change its property. We used the same trained model with Sec. 6.1, but used cross-entropy loss for calculating the Hessian and just plotted the trace norm of the Hessian without normalization (5).

Figure 4 shows the results. Even though shapness without normalization can also distinguish models trained on random labels to some extent, the signal is weaker compared to normalized sharpness. Especially, in larger models with normalization layers, sharpness without normalization lost its ability to distinguish models. This result supports the significance of the scale sensitivity problem and benefits of our modification.

7 Discussion

In this section, we discuss connections between normalized flat minima and previous studies.

7.1 Connection to MDL arguments

Minimum description length (MDL) (Rissanen, 1986) provides us with a measure of generalization through the amount of the necessary information to describe the model. Intuitively, at flat minima, we can use less accurate representations of the parameters and thus requires fewer bits. The gain of the description length is quantitatively explained by bits-back arguments (Hinton & van Camp, 1993; Honkela & Valpola, 2004). According to the theory, we can represent the model by the following number of bits.

$$\text{KL}[\mathbb{Q} \parallel \mathbb{P}]. \quad (24)$$

This is the same with the (B) term in (4). Thus, from the minimum description length principle, normalized sharpness balances the effect of the posterior variance and the number of bits we can save.

7.2 Comparison with other prior choices

Kingma et al. (2015) proposed a local reparametrization trick that removes the scale dependence of the KL term by hyperpriors. However, in Kingma et al. (2015), reparametrization was performed per parameter. This makes the constant in (7) scales with the number of parameters. Thus, even though the trick removes the scale independence, the resultant KL-term is just as good as a naive parameter counting. On the other hand, the constant in our analysis scales at most $O(hd)$ compared to their $O(h^2d)$.

7.3 Comparison with Fisher-Rao norm:

Liang et al. (2017) proposed the Fisher-Rao norm, which is defined as follows.

$$\sum_i \left(\boldsymbol{\theta}_i^2 \mathbb{E}_{z \sim \mathcal{S}} [\nabla_{\boldsymbol{\theta}_i} \mathcal{L}_z (f_{\boldsymbol{\theta}})^2] \right). \quad (25)$$

While the formulation is similar to normalized sharpness, there are three crucial differences. First, normalized sharpness uses the Hessian, not Fisher, and directly

measures curvature. Second, the Fisher-Rao norm is parameter-wise, while the normalized sharpness exploits the parameter structures in neural networks. Third, normalized sharpness takes the square root of the Frobenius norms of parameters and the Hessian. To highlight an advantage by the third difference, we consider the following network.

$$y = \text{ReLU}(W^{(1)}x) + \text{ReLU}(W^{(2)}x). \quad (26)$$

This type of connection is often found in modern networks (Xie et al., 2017; Zoph et al., 2018). We assume that the following condition is satisfied.

$$W^{(1)} = W^{(2)} = W/2. \quad (27)$$

Next, we rescale the parameters as follows.

$$y = \text{ReLU}(W'^{(1)}x) + \text{ReLU}(W'^{(2)}x), \quad (28)$$

$$W'^{(1)} = W, \quad (29)$$

$$W'^{(2)} = \mathbf{O}. \quad (30)$$

By this rescaling, the Fisher-Rao norm of the weight matrix W becomes half, while the normalized sharpness (17) is kept the same. The definition of matrix-normalized sharpness (13) is also invariant against this rescaling. This additional invariance shows that our definition better captures generalization.

8 Conclusion

We incorporated the gain by flatness into the arguments of flat minima and proposed normalized flat minima. The advantages of our definition are as follows.

- It is invariant to transformations from which the prior definitions of flatness suffered.
- It can provide tighter bounds than naive parameter countings.

Our discussion pushes forward the generalization analysis which is invariant to some obvious transformations. Experimental results suggest that the analysis is useful to distinguish overfitted models or to prevent models from overfitting.

One flaw of the normalized flat minima is that it uses Gaussian for both prior and posterior even though that is a standard practice in the literature (Hinton & van Camp, 1993; Neyshabur et al., 2018). From Draxler et al. (2018) and Izmailov et al. (2018), we known that appropriate posteriors of networks has more complex structures than Gaussians. From the menimum description length perspective, using Gaussian limits the compression algorithms of models. Recent analysis of compression algorithmns for neural networks (Blier & Ollivier, 2018) might be useful for better prior and posterior designs. Sun et al. (2019) might help to develop methods to directly calculate the KL-divergence on function space.

Acknowledgement

YT was supported by Toyota/Dwango AI scholarship. IS was supported by KAKENHI 17H04693. MS was supported by the International Research Center for Neurointelligence (WPI-IRCN) at The University of Tokyo Institutes for Advanced Study.

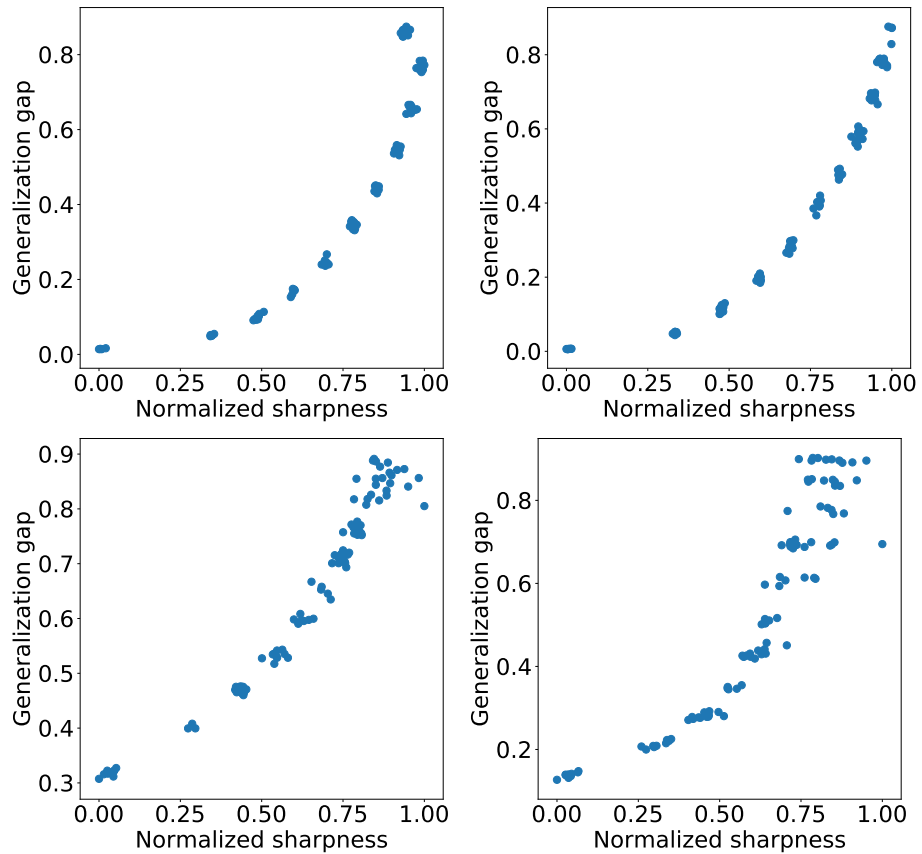


Figure 3: Scatter plot between normalized sharpness (17) and accuracy gap. Normalized sharpnesses were rescaled to $[0, 1]$ by their maximum and minimum among the trained networks. Top left figure shows the results for multi layer perceptrons on MNIST. Top right shows LeNet on MNIST. Bottom left shows LeNet on CIFAR-10. And Bottom right shows Wide ResNet on CIAFR-10.

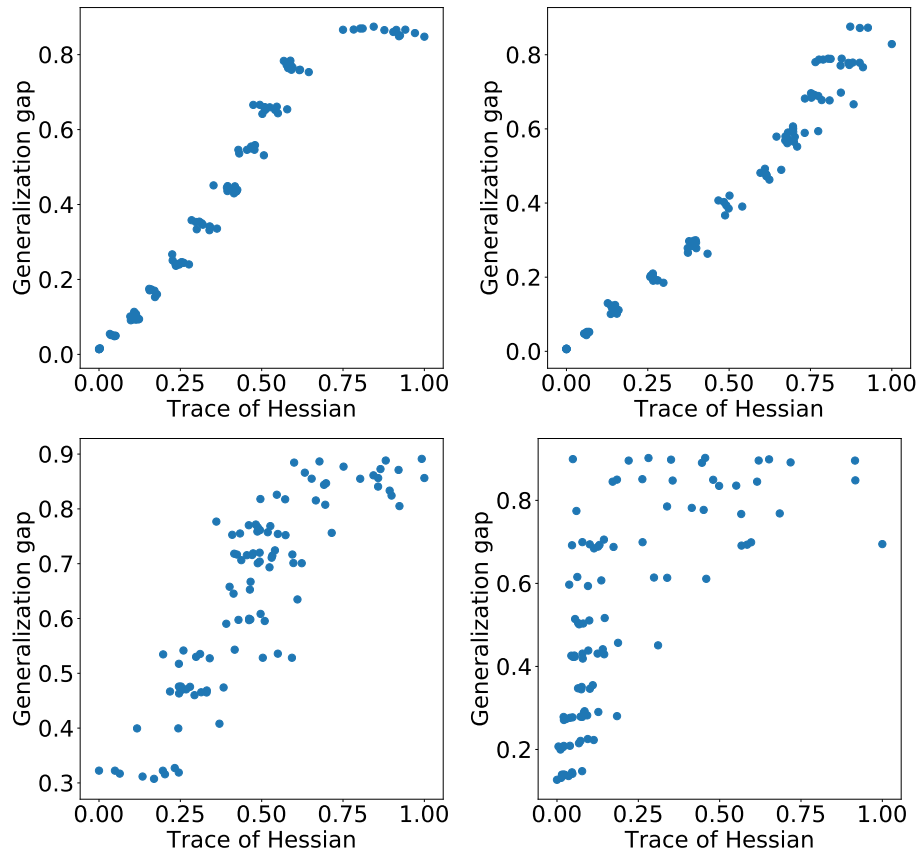


Figure 4: Scatter plot between trace of the Hessian (5) and accuracy gap. The traces were rescaled to $[0, 1]$ by their maximum and minimum among the trained networks. Top left figure shows the results for multi layer perceptrons on MNIST. Top right shows LeNet on MNIST. Bottom left shows LeNet on CIFAR-10. And Bottom right shows Wide ResNet on CIAFR-10.

References

Alquier, P., Ridgway, J., and Chopin, N. On the properties of variational approximations of Gibbs posteriors. *Journal of Machine Learning Research*, 17(239):1–41, 2016.

Arora, S., Ge, R., Neyshabur, B., and Zhang, Y. Stronger Generalization Bounds for Deep Nets via a Compression Approach. In *Proceedings of the 35th International Conference on Machine Learning*, volume 80 of *Proceedings of Machine Learning Research*, pp. 254–263. PMLR, 10–15 Jul 2018.

Bartlett, P. L., Foster, D. J., and Telgarsky, M. J. Spectrally-normalized margin bounds for neural networks. In *Advances in Neural Information Processing Systems 30*, pp. 6240–6249. Curran Associates, Inc., 2017.

Blier, L. and Ollivier, Y. The Description Length of Deep Learning Models Léonard. In *Advances in Neural Information Processing Systems 31*, pp. 2220–2230. Curran Associates, Inc., 2018.

Chaudhari, P., Choromanska, A., Soatto, S., LeCun, Y., Baldassi, C., Borgs, C., Chayes, J., Sagun, L., and Zecchina, R. Entropy-SGD: Biasing Gradient Descent Into Wide Valleys. In *International Conference on Learning Representations*, 2017.

Dinh, L., Pascanu, R., Bengio, S., and Bengio, Y. Sharp Minima Can Generalize For Deep Nets. In *Proceedings of the 34th International Conference on Machine Learning*, volume 70 of *Proceedings of Machine Learning Research*, pp. 1019–1028. PMLR, 06–11 Aug 2017.

Draxler, F., Veschgini, K., Salmhofer, M., and Hamprecht, F. Essentially no barriers in neural network energy landscape. In *Proceedings of the 35th International Conference on Machine Learning*, volume 80 of *Proceedings of Machine Learning Research*, pp. 1309–1318. PMLR, 10–15 Jul 2018.

Germain, P., Bach, F., Lacoste, A., and Lacoste-Julien, S. PAC-Bayesian Theory Meets Bayesian Inference. In *Advances in Neural Information Processing Systems 29*, pp. 1884–1892. Curran Associates, Inc., 2016.

Hinton, G. E. and van Camp, D. Keeping the Neural Networks Simple by Minimizing the Description Length of the Weights. In *Proceedings of the Sixth Annual Conference on Computational Learning Theory*, COLT '93, pp. 5–13. ACM, 1993. ISBN 0-89791-611-5.

Hochreiter, S. and Schmidhuber, J. Flat Minima. *Neural Computation*, 9(1): 1–42, 1997.

Hoffer, E., Hubara, I., and Soudry, D. Train longer, generalize better: closing the generalization gap in large batch training of neural networks. In *Advances in Neural Information Processing Systems 30*, pp. 1731–1741. Curran Associates, Inc., 2017.

Honkela, A. and Valpola, H. Variational Learning and Bits-back Coding: An Information-theoretic View to Bayesian Learning. *Trans. Neur. Netw.*, 15(4): 800–810, July 2004. ISSN 1045-9227.

Ioffe, S. and Szegedy, C. Batch Normalization: Accelerating Deep Network Training by Reducing Internal Covariate Shift. In *Proceedings of the 32nd International Conference on Machine Learning*, volume 37 of *Proceedings of Machine Learning Research*, pp. 448–456. PMLR, 07–09 Jul 2015.

Izmailov, P., Podoprikhin, D., Garipov, T., Vetrov, D. P., and Wilson, A. G. Averaging Weights Leads to Wider Optima and Better Generalization. In *Conference on Uncertainty in Artificial Intelligence*, 2018.

Keskar, N. S., Mudigere, D., Nocedal, J., Smelyanskiy, M., and Tang, P. T. P. On Large-Batch Training for Deep Learning: Generalization Gap and Sharp Minima. In *International Conference on Learning Representations*, 2017.

Kingma, D. P., Salimans, T., and Welling, M. Variational Dropout and the Local Reparameterization Trick. In *Advances in Neural Information Processing Systems 28*, pp. 2575–2583. Curran Associates, Inc., 2015.

Krizhevsky, A. Learning Multiple Layers of Features from Tiny Images. 2009.

Langford, J. and Caruana, R. (Not) Bounding the True Error. In *Advances in Neural Information Processing Systems 14*, pp. 809–816. MIT Press, 2002.

Lecun, Y., Bottou, L., Bengio, Y., and Haffner, P. Gradient-based Learning Applied to Document Recognition. In *Proceedings of the IEEE*, pp. 2278–2324, 1998.

LeCun, Y., Cortes, C., and Burges, C. J. C. The MNIST Database of Handwritten Digits. 1998.

Li, H., Xu, Z., Taylor, G., and Goldstein, T. Visualizing the Loss Landscape of Neural Nets. In *Advances in Neural Information Processing Systems 31*, pp. 6391–6401. Curran Associates, Inc., 2018.

Liang, T., Poggio, T. A., Rakhlin, A., and Stokes, J. Fisher-Rao Metric, Geometry, and Complexity of Neural Networks. *CoRR*, abs/1711.01530, 2017.

McAllester, D. A. Some PAC-Bayesian Theorems. *Machine Learning*, 37(3): 355–363, Dec 1999. ISSN 1573-0565.

McAllester, D. A. PAC-Bayesian Stochastic Model Selection. *Machine Learning*, 51(1):5–21, Apr 2003. ISSN 1573-0565.

Neyshabur, B., Bhojanapalli, S., Mcallester, D., and Srebro, N. Exploring Generalization in Deep Learning. In *Advances in Neural Information Processing Systems 30*, pp. 5947–5956. Curran Associates, Inc., 2017.

Neyshabur, B., Bhojanapalli, S., and Srebro, N. A PAC-Bayesian Approach to Spectrally-Normalized Margin Bounds for Neural Networks. In *International Conference on Learning Representations*, 2018.

Rissanen, J. Stochastic complexity and modeling. *Ann. Statist.*, 14(3):1080–1100, 09 1986.

Salimans, T. and Kingma, D. P. Weight Normalization: A Simple Reparameterization to Accelerate Training of Deep Neural Networks. In *Advances in Neural Information Processing Systems 29*, pp. 901–909. Curran Associates, Inc., 2016.

Sun, S., Zhang, G., Shi, J., and Grosse, R. Functional Variational Bayesian Neural Networks. In *International Conference on Learning Representations*, 2019.

Szegedy, C., Zaremba, W., Sutskever, I., Bruna, J., Erhan, D., Goodfellow, I., and Fergus, R. Intriguing properties of neural networks. In *International Conference on Learning Representations*, 2014.

Wang, H., Shirish Keskar, N., Xiong, C., and Socher, R. Identifying Generalization Properties in Neural Networks. *ArXiv e-prints*, 2018.

Xie, S., Girshick, R. B., Dollár, P., Tu, Z., and He, K. Aggregated Residual Transformations for Deep Neural Networks. In *2017 IEEE Conference on Computer Vision and Pattern Recognition, CVPR 2017, Honolulu, HI, USA, July 21-26, 2017*, pp. 5987–5995, 2017.

Yao, Z., Gholami, A., Lei, Q., Keutzer, K., and Mahoney, M. W. Hessian-based Analysis of Large Batch Training and Robustness to Adversaries. In *Advances in Neural Information Processing Systems 31*, pp. 4954–4964. Curran Associates, Inc., 2018.

Zagoruyko, S. and Komodakis, N. Wide Residual Networks. In *Proceedings of the British Machine Vision Conference*, pp. 87.1–87.12, 2016.

Zoph, B., Vasudevan, V., Shlens, J., and Le, Q. V. Learning Transferable Architectures for Scalable Image Recognition. In *CVPR*, pp. 8697–8710. IEEE Computer Society, 2018.

A Running examples

A.1 Row and column scaling

We show running examples of the transformation proposed in Sec. 5.1. We consider the following network.

$$f(X) = W^{(2)}(\text{ReLU}(W^{(1)}(X))), \quad (31)$$

$$W^{(1)} = \begin{pmatrix} 1 & 2 \\ 3 & 4 \end{pmatrix}, \quad (32)$$

$$W^{(2)} = \begin{pmatrix} 5 & 6 \\ 7 & 8 \end{pmatrix}. \quad (33)$$

Now, matrix norms are as follows.

$$\|W^{(1)}\|_F = \sqrt{30}, \quad (34)$$

$$\|W^{(1)}\|_2 \approx 5.48, \quad (35)$$

$$\|W^{(2)}\|_F = \sqrt{174}, \quad (36)$$

$$\|W^{(2)}\|_2 \approx 13.19. \quad (37)$$

We apply the transformation to the first row of $W^{(1)}$ and the first column of $W^{(2)}$ with $\alpha = 10$. Then, parameters change as follows.

$$W^{(1)} = \begin{pmatrix} 0.1 & 0.2 \\ 3 & 4 \end{pmatrix}, \quad (38)$$

$$W^{(2)} = \begin{pmatrix} 50 & 6 \\ 70 & 8 \end{pmatrix}. \quad (39)$$

Next, we apply the transformation to the second row of $W^{(1)}$ and the second column of $W^{(2)}$ with $\alpha = 0.1$. Parameters change as follows.

$$W^{(1)} = \begin{pmatrix} 0.1 & 0.2 \\ 30 & 40 \end{pmatrix}, \quad (40)$$

$$W^{(2)} = \begin{pmatrix} 50 & 0.6 \\ 70 & 0.8 \end{pmatrix}. \quad (41)$$

Now, matrix norms changed as follows.

$$\|W^{(1)}\|_F = \sqrt{2500.05}, \quad (42)$$

$$\|W^{(1)}\|_2 \approx 50.00, \quad (43)$$

$$\|W^{(2)}\|_F = \sqrt{6101.13}, \quad (44)$$

$$\|W^{(2)}\|_2 \approx 78.11. \quad (45)$$

Using the same method, we can make matrix norms of both $W^{(1)}$ and $W^{(2)}$ arbitrarily large.

B Convexity of variance parameters

We show that the optimization problem (17) is convex with respect to the log of variance parameters σ^2 and σ'^2 . Let us define the following parameters.

$$e^{x_i} := \sigma_i^2, \quad (46)$$

$$e^{y_j} := \sigma_j'^2. \quad (47)$$

For the sake of notational simplicity, we rewrite the objective in (17) as follows.

$$S := \sum_{i,j} (\alpha_{i,j} e^{x_i} e^{y_j} + \beta_{i,j} e^{-x_i} e^{-y_j}), \quad (48)$$

where $\alpha_{i,j} \geq 0$ and $\beta_{i,j} \geq 0$ for all i and j . To show that S is convex with respect to \mathbf{x} and \mathbf{y} , we show that the Hessian of S is semi-positive definite. First, we calculate the elements of the Hessian.

$$\frac{\partial^2 S}{\partial x_i \partial x_j} = \sum_k (\alpha_{i,k} e^{x_i} e^{y_k} + \beta_{i,k} e^{-x_i} e^{-y_k}) \delta_{i,j}, \quad (49)$$

$$\frac{\partial^2 S}{\partial y_i \partial y_j} = \sum_k (\alpha_{k,j} e^{x_k} e^{y_j} + \beta_{k,j} e^{-x_k} e^{-y_j}) \delta_{i,j}, \quad (50)$$

$$\frac{\partial^2 S}{\partial x_i \partial y_j} = \alpha_{i,j} e^{x_i} e^{y_j} + \beta_{i,j} e^{-x_i} e^{-y_j}. \quad (51)$$

For the notational simplicity, we define the following.

$$\gamma_{i,j} := \alpha_{i,j} e^{x_i} e^{y_j} + \beta_{i,j} e^{-x_i} e^{-y_j}. \quad (52)$$

Note that $\gamma \geq 0$. We can rewrite the elements of the Hessian as follows.

$$\frac{\partial^2 S}{\partial x_i \partial x_j} = \sum_k \gamma_{i,k} \delta_{i,j}, \quad (53)$$

$$\frac{\partial^2 S}{\partial y_i \partial y_j} = \sum_k \gamma_{k,j} \delta_{i,j}, \quad (54)$$

$$\frac{\partial^2 S}{\partial x_i \partial y_j} = \gamma_{i,j}. \quad (55)$$

Now, it suffices to show that $\forall v, v^\top (\nabla_{\mathbf{x}, \mathbf{y}}^2 S) v \geq 0$.

$$v^\top (\nabla_{\mathbf{x}, \mathbf{y}}^2 S) v \quad (56)$$

$$= \sum_{i,j} (\gamma_{i,j} v_{x_i}^2) + \sum_{i,j} (\gamma_{i,j} v_{y_j}^2) + 2 \sum_{i,j} \gamma_{i,j} v_{x_i} v_{y_j} \quad (57)$$

$$= \sum_{i,j} \gamma_{i,j} (v_{x_i} + v_{y_j})^2 \geq 0 \quad \square \quad (58)$$

C Calculation of normalized sharpness

To calculate the normalized flat minima (17), we have to solve the following optimization problem for each weight matrix.

$$\min_{\sigma, \sigma'} \sum_{i,j} \left(\frac{\partial^2 \mathcal{L}_S(f_\theta)}{\partial W_{i,j} \partial W_{i,j}} (\sigma_i \sigma'_j)^2 + \frac{W_{i,j}^2}{2\lambda(\sigma_i \sigma'_j)^2} \right). \quad (59)$$

The parameter λ is arbitrary but we set $\lambda = 1$ for simplicity. If we can estimate the diagonal elements of the Hessian, the later parts are straightforward. We can use the following to estimate the diagonal elements of the Hessian.

$$\mathbb{E}_{\epsilon \sim \mathcal{N}(\mathbf{0}, \mathbf{1})} [\epsilon \odot \nabla_\theta^2 \mathcal{L}_S(f_\theta) \epsilon] \quad (60)$$

$$\approx \mathbb{E}_{\epsilon \sim \mathcal{N}(\mathbf{0}, \mathbf{1})} \left[\epsilon \odot \frac{\nabla_\theta \mathcal{L}_S(f_{\theta+r\epsilon}) - \nabla_\theta \mathcal{L}_S(f_{\theta-r\epsilon})}{2r} \right], \quad (61)$$

where $r > 0$ is a small constant. In our experiments, r was chosen per weight matrix according to their Frobenius norm for better estimation of the Hessian.

D Alternative definition of the normalized sharpness

As an alternative to (17), we can directly solve the following optimization problem in (4).

$$\min_{\sigma, \sigma'} \left((\mathcal{L}_S(\mathbb{Q}_{\sigma, \sigma'}) - \mathcal{L}_S(f)) + \sum_{i,j,k} \frac{(W^{(k)}[i, j])^2}{2\lambda(\sigma_i^{(k)} \sigma_j'^{(k)})^2} \right). \quad (62)$$

We can use stochastic gradient descent to optimize σ and σ' . An advantage of (62) over (17) is that we do not need a second-order approximation. However, we have the following disadvantages.

- The optimization problem becomes nonconvex.
- Sharpness becomes sensitive to the choice of λ ⁷.

Given these disadvantages of (62), we use (17) as a definition of the normalized sharpness.

⁷The quantity (17) is invariant to the choice of λ in a sense that sharper model is always sharper no matter which λ we set. On the other hand, the quantity (62) does not have the invariance.

E Experimental setups

E.1 Setups of Sec. 6.1

Ratio of random labels were selected from (0.0, 0.1, 0.2, 0.3, 0.4, 0.5, 0.6, 0.7, 0.8, 0.9, 1.0) uniform randomly at each training. We used cross entropy loss during the training. We used normalized-softmax-cross-entropy loss (20) to calculate normalized sharpness.

MLP on MNIST: We trained MLP for 50 epochs with batchsize 128 on MNIST. We used Adam optimizer with its default parameters (lr = 0.001).

LeNet on MNIST: We trained LeNet for 50 epochs with batchsize 128 on MNIST. We used Adam optimizer with its default parameters (lr = 0.001).

LeNet on CIFAR10: We trained LeNet for 100 epochs with batchsize 128 on CIFAR10. We used Adam optimizer with its default parameters (lr = 0.001).

Wide ResNet on CIFAR10: We trained 16 layers Wide ResNet for 200 epochs with batchsize 128 on CIFAR10. We used width factor $k = 4$. We used Adam optimizer with its default parameters (lr = 0.001).

E.2 Setups of Sec. 6.2

We used the same setups described in Sec. E.2. We used cross entropy loss for both training and calculation of the Hessian.